

## The anomalous diffusion of biological water provides microstructural and physiological information of brain tissue

Alessandra Caporale<sup>ab</sup>, Marco Palombo<sup>c</sup>, Emiliano Macaluso<sup>d</sup>, Michele Guerreri<sup>ae</sup>, Marco Bozzali<sup>f</sup>, and Silvia Capuani<sup>a</sup>

<sup>a</sup> CNR ISC UOS Roma Sapienza, Sapienza University of Rome, Rome, 00185, Italy

<sup>b</sup> SAIMLAL Dept., Morpho-functional Sciences, Sapienza University of Rome, Rome, Italy

<sup>c</sup> MIRCen, Commissariat à l'Energie Atomique, Fountain Aux Roses, France

<sup>d</sup> ImpAct Team, Lyon Neuroscience Research Center, Lyon, France

<sup>e</sup> SAIMLAL Dept., Morphogenesis & Tissue Engineering, Sapienza University of Rome, Rome, Italy

<sup>f</sup> NeuroImaging Laboratory, Santa Lucia Foundation, Rome, Italy

e-mail: [alessandra.stella.caporale@gmail.com](mailto:alessandra.stella.caporale@gmail.com)

Keywords: anomalous diffusion, magnetic susceptibility, MRI, relaxometry, brain

The purpose of this study is to investigate the capability of Anomalous Diffusion(AD)-MRI technique to provide additional information with respect to the conventional Gaussian diffusion techniques, regarding the microstructure and the physiology of brain tissue.

The spatial arrangement of myelinated fibers in white matter (WM) and the physiological concentrations of iron and iron storage proteins in the cortical and sub-cortical structures in gray matter (GM) cause local differences in magnetic properties among brain regions<sup>1,2</sup>, such as magnetic susceptibility differences ( $\Delta\chi$ ). The  $\Delta\chi$  distribution may reflect the health state of the brain, practically a combination of myelin integrity and iron balance. Among the MRI parameters the rate of relaxation ( $R2^*=1/T2^*$ ) is pretty sensitive to magnetic field inhomogeneity, and thus to  $\Delta\chi$ <sup>3,4</sup>.

Regarding water diffusion, the conventional diffusion techniques, such as Diffusion Tensor Imaging (DTI) can highlight the anisotropy of myelinated fibers, presenting however a limited sensitivity with respect to tissue microstructure. Indeed, the multiplicity of scale lengths and compartments characterizing brain tissue cause a deviation of water behavior from the prediction of Gaussian diffusion techniques. The AD-MRI refers instead to the Continuous Time Random Walk<sup>5</sup> model, which describes the statistics of water diffusion in complex environments, and it consists in performing a stretched-exponential fitting of Diffusion-Weighted (DW) data, collected at increasing diffusion gradient strengths. We recently highlighted that AD stretched exponent  $\gamma$  quantifies super-diffusion processes<sup>6,7</sup>, due to the internal gradients ( $G_{in}$ ) originated by  $\Delta\chi$  at the interfaces between diffusion compartments.

In our study we compared parameters derived from AD- $\gamma$  maps with  $R2^*$  in 8 healthy volunteers (4 males/4 females, mean age $\pm$ SD=25 $\pm$ 1years). MRI was performed at 3.0 T at Siemens Allegra Magnetom Scanner (Siemens Medical Solutions, Erlangen, Germany), equipped with a circularly polarized transmit-receive coil. T2\*-weighted images (T2\*WIs) were collected at TE = (10,20,35,55) ms with Echo Planar Imaging (EPI); DW-images (DWIs) were collected using 20 diffusion directions and b-values (0,100,200,300,400,500,700,800,1000,1500,2000,2500,3000,4000,5000) s/mm<sup>2</sup>, with a DW-Double-Spin-Echo-EPI (TR/TE=6400ms/107ms;  $\Delta\delta=72$ ms/35ms). 32 axial slices 3mm-thick, parallel to the anterior-posterior commissure were acquired in anterior-posterior direction (matrix size=128x128, in-plane resolution=1.8x1.8 mm<sup>2</sup>). Signal-to-Noise Ratio of DWIs was approximately 55 for gray matter (GM), 25 for white matter (WM), and it was above 4 for the highest b-value, ensuring the reliability of DW-data<sup>8</sup>.

We calculated rotationally invariant  $\gamma$ -metrics (mean- $\gamma$ ,  $M\gamma$ ; axial- $\gamma$ ,  $\gamma_{//}$ ; radial- $\gamma_{\perp}$ ;  $\gamma$ -anisotropy,  $A\gamma$ ), similarly to the DTI approach<sup>9</sup>. We extracted Regions of Interest (ROIs) in WM and GM using atlases in subject's native space (Fig. 1), computing the relative mean values $\pm$ SD.  $\Delta\chi$  values<sup>1</sup> and iron concentrations ([Fe]) of GM ROIs<sup>10</sup> were taken from literature. Pearson's correlation tests were performed, with P-values<0.05 considered as statistically significant.

We found a significant linear correlation between  $R2^*$  and the fibers orientation angle  $\Phi$  in WM ( $r=-0.381, P<0.0001$ ), and a strong linear correlation ( $r=-0.950, P=0.05$ ) between  $R2^*$  and [Fe] in GM, in agreement with literature<sup>6,7</sup> (Fig. 2), proving that  $R2^*$  reflected  $\Delta\chi$  inhomogeneity in WM and GM, and justifying the study of the dependence of on  $\Delta\chi$  through the investigation of its dependence on  $R2^*$ .

In both WM ROIs and GM ROIs strong negative correlations between AD-metrics and  $R2^*$  were found (respectively, in WM  $M\gamma$ :  $r=-0.786, P=0.022$ ;  $\gamma_{//}$ :  $r=-0.822, P=0.012$ ; in GM  $M\gamma$ :  $r=-0.997, P=0.003$ ;  $\gamma_{\perp}$ :  $r=-0.989, P=0.011$ ), while DTI-metrics did not correlate with  $R2^*$  (Fig. 3).

Furthermore, we found a negative linear trend between  $R2^*$  and  $\Delta\chi$  in WM ROIs, a positive linear trend in GM ROIs, and an opposite trend of AD-parameters vs  $\Delta\chi$  compared to  $R2^*$  (Fig. 4).

In conclusion this work, confirming results obtained in vitro<sup>3,4</sup>, suggested that AD-metrics, differently from DTI, reflects  $\Delta\chi$  due to differences in myelin orientation and iron content within selected regions in WM and GM at 3.0 T. This may have a clinical impact in the field of neuroimaging aimed at monitoring both myelin integrity and alterations due to abnormal iron accumulation, which is associated to oxidative stress and neurodegenerative processes in human brain<sup>11</sup>.

- [1] W. Li et al., Neuroimage 59(3) (2012) 2088-97.
- [2] W. Li et al., Neuroimage 55(4) (2014) 1645-1656.
- [3] D.A. Rudko et al., PNAS 111(1) (2014) E159-E167.
- [4] N.J Gelman et al., Radiology 210(3) (1999) 759-767.
- [5] R. Metzler, J. Klafter, Phys. Rep. 339 (2000) 1–77.
- [6] M. Palombo et al., JMRI 216 (2012) 28-36.
- [7] G. Di Pietro et al., App Magn Res 45(8) (2014) 771-784.
- [8] D.K. Jones et al., Neuroimage 73 (2013) 239-254.
- [9] S. De Santis et al., MRM 64(4) (2011) 1043-1052.
- [10] B. Hallgren and P. Sourander J of Neurochem 3(1) (1958) 41-51.
- [11] L. Zecca et al., Nature Rev Neurosci 5(11) (2004) 863-873.

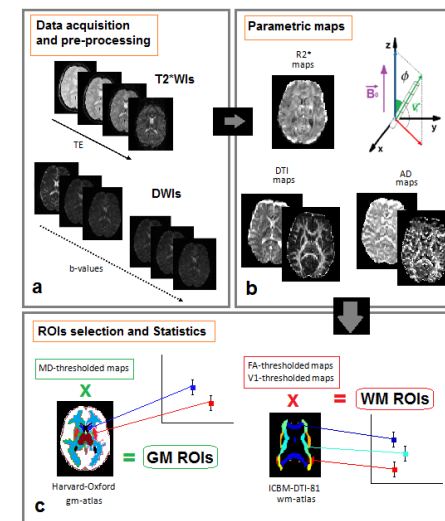


Figure 1 - Flow-chart illustrating the methods. a) Pre-processing of the acquired images, and extraction of parametric maps. b) The orientation of WM fibers  $\Phi$  with respect to the magnetic field was estimated using

trigonometric relations. c) A composition of thresholds on parametric maps and the use of standard atlases was adopted for WM and GM ROIs selection.

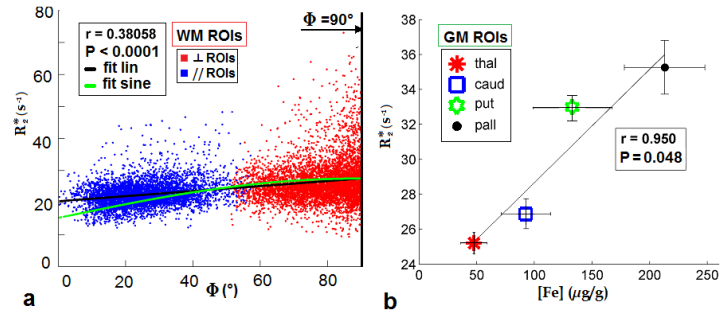


Figure 2 -  $R_2^*$  dependence on magnetic inhomogeneity in WM and GM. a)  $R_2^*$  of WM ROIs with parallel fibers (blue dots) and orthogonal fibers (red dots), plotted against their orientation. The data are linearly fitted (black line), and fitted with a sine function (green curve). b)  $R_2^*$  of thalamus (thal), caudate nuclei (caud), putamen (put) and globus pallidus (pall), estimated from the parametric  $R_2^*$  maps and plotted vs non-heme iron contents. Pearson's correlation coefficient  $r$  is reported in the box, together with the level of significance,  $P$ .

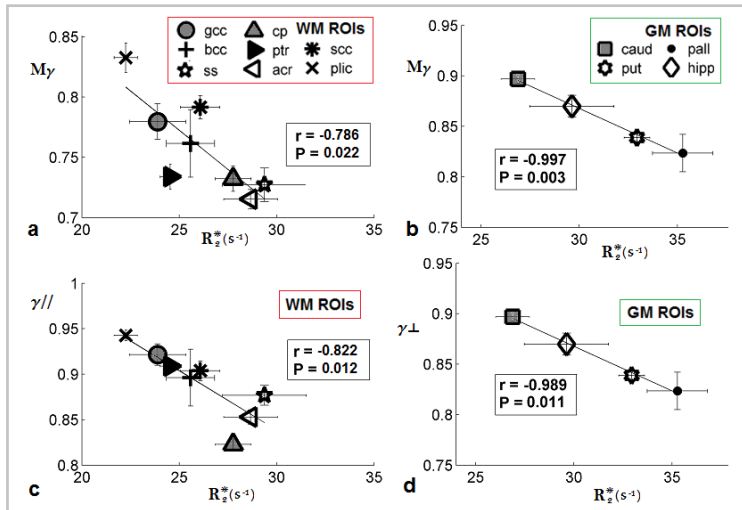


Figure 3 - AD-metrics plotted vs  $R_2^*$ . Mean values of mean- $\gamma$  ( $M\gamma$ ), axial- $\gamma$  ( $\gamma_{//}$ ) in WM-ROIs (a,c) and of  $M\gamma$  and radial- $\gamma$  ( $\gamma_{\perp}$ ), as a function of  $R_2^*$  in GM-ROIs (b,d). Error bars indicate inter-subjects SD; the linear fit, Pearson's correlation coefficient and the significance level are indicated (gcc=genu of corpus callosum, cc; bcc=body of cc; sec=splenium of cc; plic=posterior limb of internal capsule; cp=cerebral

peduncle; ptr=posterior thalamic radiations; acr=anterior corona radiata; ss=sagittal stratum; caud=caudate; put=putamen; pall=pallidum; hipp=hippocampus).

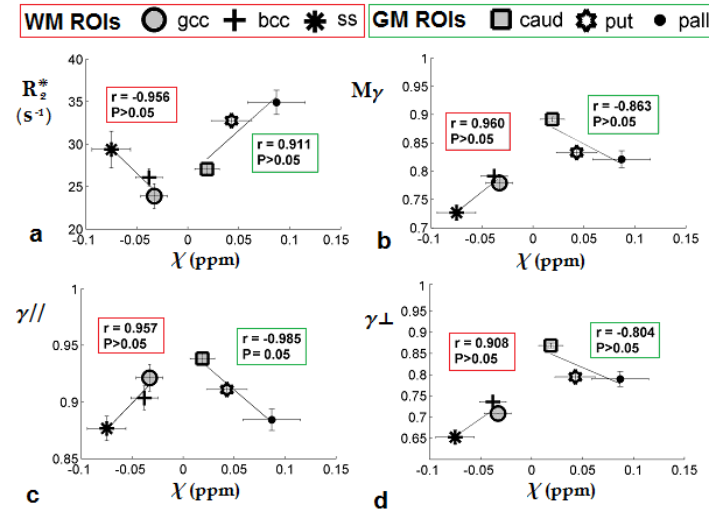


Figure 4 -  $R_2^*$  and AD-derived parameters plotted against  $\chi$  in WM and GM ROIs. The trends are indicated by linear fits, that are treated separately for WM and GM ROIs. Pearson's correlation coefficients,  $r$ , are reported in the boxes, together with the level of significance,  $P$  (red boxes for WM ROIs; green boxes for GM ROIs; gcc=genu of corpus callosum, cc; bcc=body of cc; ss=sagittal stratum; caud=caudate; put=putamen; pall=pallidum).

### Synopsis

This study aimed at investigating the capability of Anomalous Diffusion(AD)-MRI technique to provide complementary information with respect to the conventional diffusion techniques, regarding the microstructure of brain tissue. Here we confirmed *in vivo* the results previously obtained *in vitro*, suggesting that AD-MRI, differently from DTI, reflects magnetic susceptibility differences due to differences in myelin orientation and iron content within selected regions in brain parenchyma.